Theoretical approach for computing magnetic anisotropy in single molecule magnets

Rajamani Raghunathan,[1] S. Ramasesha,[1,*] and Diptiman Sen[2]
[1]*Solid State and Structural Chemistry Unit, Indian Institute of Science, Bangalore 560012, India*
[2]*Centre for High Energy Physics, Indian Institute of Science, Bangalore 560012, India*
(Received 30 May 2008; published 16 September 2008)

We present a theoretical approach to calculate the molecular magnetic anisotropy parameters, D_M and E_M for single molecule magnets in any eigenstate of the exchange Hamiltonian, treating the anisotropy Hamiltonian as a perturbation. Neglecting intersite dipolar interactions, we calculate molecular magnetic anisotropy in a given total spin state from the known single-ion anisotropies of the transition metal centers. The method is applied to $Mn_{12}Ac$ and Fe_8 in their ground and first few excited eigenstates, as an illustration. We have also studied the effect of orientation of local anisotropies on the molecular anisotropy in various eigenstates of the exchange Hamiltonian. We find that, in case of $Mn_{12}Ac$, the molecular anisotropy depends strongly on the orientation of the local anisotropies and the spin of the state. The D_M value of $Mn_{12}Ac$ is almost independent of the orientation of the local anisotropy of the core Mn(IV) ions. In the case of Fe_8, the dependence of molecular anisotropy on the spin of the state in question is weaker. We have also calculated the anisotropy constants for several sets of exchange parameters and found that in $Mn_{12}Ac$ the anisotropy increases with spin excitation gap, while in Fe_8, the anisotropy is almost independent of the gap.

DOI: 10.1103/PhysRevB.78.104408 PACS number(s): 75.50.Xx, 75.30.Gw

I. INTRODUCTION

Following the synthesis and the discovery of exotic properties such as quantum resonant tunneling (QRT) in the single molecule magnet (SMM) $Mn_{12}Ac$ during the 1990s, there has been a flurry of activity in the field of molecular magnetism.[1–4] This has led to the synthesis of new systems such as Fe_8, as well as to the observation of new phenomena such as quantum coherence.[5,6] SMMs are mainly high nuclearity transition metal complexes with a high spin ground state (S_{GS}). They are also characterized by large uniaxial magnetic anisotropy.[7] The Hamiltonian corresponding to the magnetic anisotropy of a molecular system can be written as

$$\hat{H}_D = \hat{S}_M \cdot \mathcal{D}^{(M)} \cdot \hat{S}_M, \tag{1}$$

where $\hat{S}_M$ is the spin operator for the total spin of the molecule and $\mathcal{D}^{(M)}$ is the magnetic anisotropy tensor of the molecule. In usual practice, the anisotropy tensor is diagonalized and the principal axis of the molecule would correspond to the eigenvectors of the tensor. Since in most physical situations, the quantity of interest is the energy gaps between the otherwise degenerate states split by the magnetic anisotropy, the condition of zero trace is imposed on the $\mathcal{D}^{(M)}$ tensor. If D^M_{XX}, D^M_{YY}, and D^M_{ZZ} are the molecular anisotropies along the three principal directions such that $D^M_{XX}+D^M_{YY}+D^M_{ZZ}=0$, we can define two parameters, D_M and E_M, given by

$$D_M = D^M_{ZZ} - \frac{1}{2}(D^M_{XX} + D^M_{YY}),$$

$$E_M = \frac{1}{2}(D^M_{XX} - D^M_{YY}),$$

where D_M and E_M are called the axial and rhombic anisotropies, respectively. This leads to the common form of the magnetic anisotropy Hamiltonian of a SMM,

$$\hat{H}_M = D_M\left(\hat{S}^2_Z - \frac{1}{3}S(S+1)\right) + E_M(\hat{S}^2_X - \hat{S}^2_Y). \tag{2}$$

For the single molecule magnet to have nonzero magnetization in the ground state, it is necessary that the anisotropy constant D_M in the spin Hamiltonian [Eq. (2)] of the complex be negative; this ensures that the ground state of the system then would correspond to the highest magnetization state of the molecule, in its high spin ground state. This requirement of negative D_M, besides a high spin ground state, makes it hard to tailor the SMMs. The second-order transverse or rhombic anisotropy given by the last term in Eq. (2) allows transition between states with spin S that differ in their M_s values by two. E_M will be zero if the $S^2_X - S^2_Y$ operator does not remain invariant under symmetry of the molecule. In this case higher-order spin-spin interaction terms are required to observe the QRT. For example, the D_{2d} symmetry in $Mn_{12}Ac$ prohibits the existence of first-order rhombic anisotropy. Thus, the parameters D_M and E_M govern the quantum tunneling properties of a SMM, and inputs from theoretical modeling could help in designing the architecture for the synthesis of SMMs.

Theoretical modeling of SMMs presents two difficulties. First, the complexes contain many spin centers, and often these centers have different spins as in the case of $Mn_{12}Ac$, where the four Mn(IV) ions have spin-3/2, while the eight Mn(III) ions have spin-2. In these systems, usually there exist multiple exchange pathways between any given pair of ions leading to uncertain magnitude and sign of the magnetic interactions in the system. The topology of magnetic interactions often results in magnetic frustration, leading to closely spaced low-lying states of unpredictable total spin. Thus, solving even the simple Heisenberg exchange Hamiltonian of these systems turns out to be a challenge. If we do not employ a spin adapted basis to set up the Hamiltonian matrix, we could encounter convergence difficulties associated with closely spaced eigenvalues even when the correspond-

ing eigenstates belong to different total spin sectors. However, the assorted spin cluster, which a SMM is, renders construction of spin adapted basis difficult. This problem has been addressed by resorting to a valence-bond scheme for construction of the spin adapted basis, and we are now in a position to block diagonalize the Hamiltonian by exploiting both spin and spatial symmetries.[8] Thus, while the challenge of accurately solving the exchange Hamiltonian of a large assorted spin system with arbitrary topology of exchange interactions is within grasp, the challenge of computing the magnetic anisotropy constants of a SMM still remains.

The magnetic anisotropy in an isolated ion arises from explicit dipolar interactions between the unpaired electrons in the magnetic center, as well as from relativistic (spin-orbit) interactions. The former is the main origin of zero-field splitting observed in triplet states of conjugated organic molecules such as naphthalene.[10] However, in systems containing heavier elements the relativistic effects dominate. In a system with several magnetic centers such as a SMM, given the spin and single-ion anisotropy of each magnetic center, the magnetic anisotropy could arise both from dipolar interactions between magnetic centers and relativistic effects. The usual approach in these cases is to carry out simple tensoral summation of the anisotropies of the constituent magnetic centers to obtain the magnetic anisotropy in the SMMs along the lines of an oriented gas model employed in the calculation of macroscopic nonlinear optic (NLO) coefficients from isolated molecular NLO coefficients.[11–13] Such an approach, in the case of SMMs, suffers from the drawback that the anisotropy constants so computed are independent of the total spin state of the molecule.

There have been several earlier works on the computation of anisotropy tensor $\mathcal{D}^{(M)}$ of SMMs.[14–18] These approaches are based on density-functional methods. The effective mean-field Hamiltonian for the magnetic cluster is obtained in the density functional theory (DFT) formalism with desired S_z^{total} of the cluster. Besides, it is also ensured that the individual magnetic centers have the observed local spin by enforcing the z component of the ion to be equal to the known spin of the ion. From the resulting potential $\Phi(r)$, the spin-orbit (SO) operator $\hat{S}\cdot[\hat{p}\times\vec{\nabla}\Phi(\vec{r})]$ is treated as a perturbation in second order, and the anisotropy constants are extracted. This approach has some drawbacks. It is well known that the DFT method does not conserve total spin and the ground state has admixture of many spin states. Thus, it is not guaranteed that the calculations are done on the $S^{\text{total}}=10$ ground state of the Mn_{12} cluster. Besides, the method also does not guarantee that the spins on the local centers are correctly conserved. While the DFT method may give the correct local single-ion anisotropy, it is unlikely that the anisotropy of the full cluster will be obtained accurately as the latter is determined by spin-spin correlations, and mean-field theories do not give correct spin correlations. In the case of single-ions, Neese and Solomon[19] have restricted configuration interaction approach, which appears to yield correct single-ion anisotropy.

In the electron paramagnetic resonance (EPR) studies involving a pair of high spin ions, a perturbation approach was developed by Bencini and Gatteschi[13] to obtain the anisotropy of the total system, knowing the anisotropy constants of two individual ions. This method is purely analytical since they dealt with only two magnetic ions. In this paper, we develop a general methodology to deal with large cluster of ions with arbitrary spins in any given total spin state. We use a spin-exchange Hamiltonian to describe the cluster, unlike the all electron Hamiltonian that is employed in DFT studies. We obtain desired exact eigenstates of the exchange Hamiltonian, using the magnetic anisotropic interactions as a perturbation, and compute the molecular anisotropy constants in the desired eigenstates, in first-order perturbation. The input parameters required in our study are the local single-ion anisotropies and the exchange constants of the exchange Hamiltonian. Our study can yield the anisotropy values for different total spin states, as well as for different states with the same total spin. In Sec. II we describe the method in detail. In Sec. III we present the results of our studies on the two SMMs, Mn_{12}Ac and Fe_8. In Sec. IV we summarize our studies.

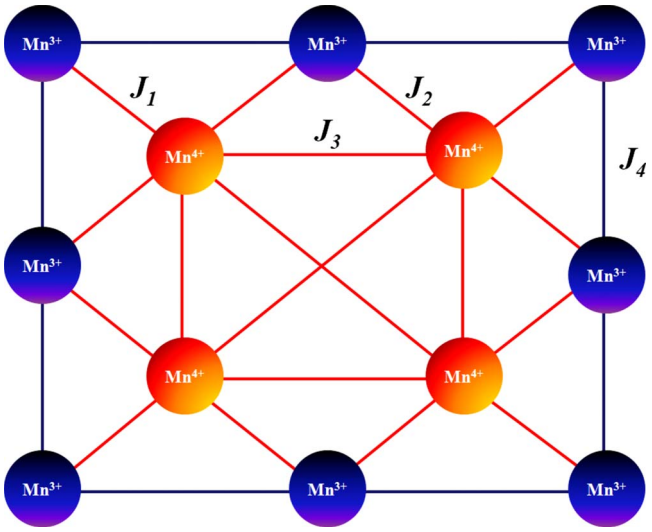

FIG. 1. (Color online) Schematic of possible exchange interactions in Mn_{12}Ac SMM. The peripheral ions are Mn(III) with spin-2 and the interior ions are Mn(IV) with spin-3/2. Js are the strength of superexchange interaction with $J_1=215$ K, $J_2=J_3=85.6$ K, and $J_4=-64.5$ K (Ref. 9).

II. FORMULATION OF THE METHOD

We treat the exchange Hamiltonian between magnetic centers in the SMMs as the unperturbed Hamiltonian,

$$\hat{H}_0=\sum_{\langle ij\rangle}J_{ij}\hat{S}_i\cdot\hat{S}_j, \tag{3}$$

where $\langle ij\rangle$ runs over all pairs of centers in the model for which the exchange constant is nonzero and $\hat{S}_i$ is the spin on the ith magnetic center. In SMMs, such as Mn_{12}Ac, the spins at all the magnetic centers are not the same and the exchange interactions are shown in Fig. 1. H_0 can be solved exactly for a few low-lying states in a chosen spin sector by using methods that have been described in detail elsewhere.[9]

The general anisotropic interactions in a collection of magnetic centers is treated as a perturbation with Hamiltonian $\hat{H}_1'$ given by

$$\hat{H}_1' = \frac{1}{2}\sum_i \sum_j \sum_\alpha \sum_\beta D_{ij,\alpha\beta}\hat{S}_i^\alpha \hat{S}_j^\beta, \tag{4}$$

where the indices i and j run over all the magnetic centers, and α and β run over x, y, and z directions of the ion. The contributions to intercenter anisotropy constant arise due to dipolar interaction between the spins on the two centers, as well as due to relativistic effects. In the former, $D_{ij,\alpha\beta}$ is given by

$$D_{ij,\alpha\beta} = \frac{1}{2}g^2\mu_B^2\left\langle \frac{\mathcal{R}_{ij}^2\delta_{\alpha\beta} - 3R_{ij,\alpha}R_{ij,\beta}}{R_{ij}^5} \right\rangle, \tag{5}$$

where $\mathcal{R}_{ij}(R_{ij})$ is the vector (distance) between the magnetic centers i and j, g is the gyromagnetic ratio, and μ_B is the electronic Bohr magneton; the expectation value in Eq. (5) is obtained by integration over spatial coordinates.[20] Approximating the expectation values of the distances by the equilibrium distances, $D_{ij,\alpha\beta}$ in Eq. (5) and computing the necessary spin-spin correlation functions, we can obtain the molecular $\mathcal{D}_{\alpha\beta}^{(M)}$ tensor.[21] The eigenvalues of this matrix give the principal anisotropy values, and imposing the condition of zero trace of the matrix yields molecular magnetic anisotropy constants due to spin-spin interactions. Our computation of the magnetic anisotropy constants, assuming only spin-dipolar interactions for the SMMs $Mn_{12}Ac$ and Fe_8, gives negligible values of the anisotropy constants compared to the experimental values of $D_M = -0.7$ and -0.28 K, respectively, in the $S=10$ ground state.[22,23] Hence in what follows, we completely neglect the contribution of spin-dipolar interactions and focus only on the magnetic anisotropy of the SMMs arising from the anisotropy of individual magnetic centers. The latter is a consequence of mainly spin-orbit interactions. We now assume that the interactions responsible for magnetic anisotropy are short ranged, and we neglect intercenter contributions to magnetic anisotropy in Eq. (4). This is justified since relativistic (spin-orbit) interactions, largely responsible for the anisotropy, is short ranged (falling off as $1/r^3$) and the distances between the magnetic centers is much larger compared to the ionic radius of the transition metal ion. The resulting perturbation term is given by

$$\hat{H}_1 = \sum_i \sum_\alpha \sum_\beta D_{i,\alpha\beta}\hat{S}_i^\alpha \hat{S}_i^\beta, \tag{6}$$

where only on-site terms are retained. If the individual magnetic centers have different principal axes, then we choose a laboratory frame and project the local tensor components on to the laboratory frame. In such a case, Eq. (6) is modified to

$$\hat{H}_1 = \sum_i \sum_\alpha \sum_\beta \sum_l \sum_m C_{i,l\alpha}C_{i,m\beta}D_{i,\alpha\beta}\hat{S}_i^\alpha \hat{S}_i^\beta, \tag{7}$$

where $C_{i,l\alpha}$ are the direction cosines of the local axis of the ith magnetic center with the $l(m)$ being the coordinate of the laboratory frame and $\alpha(\beta)$ being the local coordinates. Since the Hamiltonians in Eqs. (1) and (7) are equivalent, we can equate the matrix elements $\langle n, S_M, M|\hat{H}_1|n, S_M, M'\rangle$ and $\langle S_M, M|\hat{H}_M|S_M, M'\rangle$ for any pair of eigenstates of the exchange Hamiltonian in Eq. (3); $|M\rangle$ and $|M'\rangle$ correspond to a state n with spin S_M in which we are interested. Calculating these matrix elements for $\hat{H}_M$ is straightforward from the algebra of spin operators. However, evaluation of these matrix elements between eigenstates of $\hat{H}_0$ requires a computation in the basis of the spin orientation of the sites. From a given eigenstate of $\hat{H}_0, |n, S, M\rangle$, we can compute all eigenstates with different M values by using ladder operators corresponding to spin S. Given a S value, the above condition would give rise to $(2S+1)^2$ equations, while the tensor $\mathcal{D}^{(M)}$ has only nine components. Thus, for the $Mn_{12}Ac$ system, with ground-state spin of 10, there would be 441 equations, and we will have more equations than unknowns. However, we could take any nine equations and solve for the components of the tensor $\mathcal{D}^{(M)}$, and we would get unique values of the components. This is guaranteed by the Wigner-Eckart theorem, and we have also verified this by solving for the $\mathcal{D}^{(M)}$ tensor from several arbitrarily different selections of the nine equations.

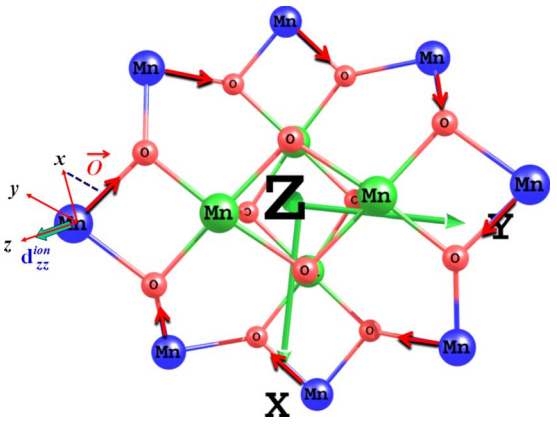

FIG. 2. (Color online) Schematic of local (x, y, and z) and laboratory (X, Y, and Z) coordinate axes in $Mn_{12}Ac$. The Mn(III) (spin-2), Mn(IV) (spin-3/2) and oxygen ions are marked in the figure. The arrows indicate the Mn-O bonds on which the chosen local x axis has maximum projection.

III. RESULTS AND DISCUSSION

We have computed D_M and E_M values for both $Mn_{12}Ac$ and Fe_8 systems for different orientations of local anisotropy.

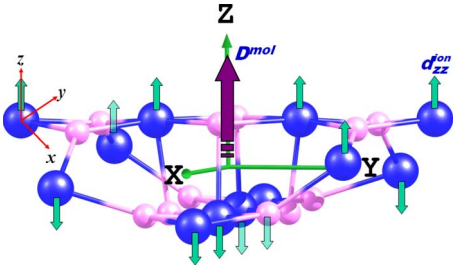

FIG. 3. (Color online) Schematic diagram showing the directions of local anisotropy in $Mn_{12}Ac$. The single-ion anisotropies of all the Mn ions are directed along the laboratory Z axis (scheme 1).

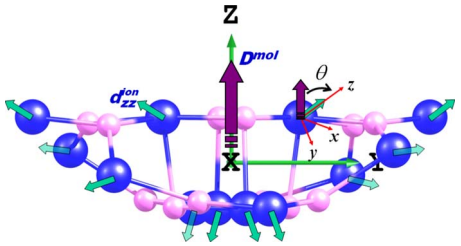

FIG. 4. (Color online) Schematic diagram showing the directions of local anisotropy in $Mn_{12}Ac$. The z component of the single-ion anisotropies of all the Mn(III) ions are inclined at an angle θ to the laboratory Z, while that of the Mn(IV) ions are kept fixed at $\sim 48°$ (scheme 2).

We have used the single-ion anisotropy values quoted in the literature for complexes of these ions in similar ligand environments.[24–27] While discussing the results, we refer to the local axes of the ions as x, y, and z, and the laboratory axes are denoted as X, Y, and Z (see Fig. 2). The laboratory frame we choose can be arbitrary. This is because, on determining $\mathcal{D}^{(M)}$ in the laboratory frame, we diagonalize it and the principal axis of the molecule is given by the eigenvectors of the $\mathcal{D}^{(M)}$ matrix. The principal axes of the molecule are unique and do not depend on the laboratory frame that is selected. We have computed the anisotropy parameters for both these systems as a function of the angle θ, which the z axis of the ion makes with the laboratory Z axis. The orientation of z component of the single-ion anisotropy in every site is shown in Figs. 3–5 (schemes 1, 2, and 3) for $Mn_{12}Ac$ and in Figs. 9–11 (schemes 4, 5, and 6) for Fe_8 systems, respectively. Once the z axis ($\vec{z}$) of the ion is fixed, then $\vec{x}$ is obtained by Gram-Schmidt orthogonalization procedure. Although the choice of this vector is arbitrary in a plane perpendicular to z axis, we have fixed the direction of $\vec{x}$ such as to have maximum projection along a M-O (M=Mn,Fe) bond in $Mn_{12}Ac$ as well as in Fe_8 (s. 2 and 11). If $\vec{O}$ is the vector connecting a M site and a neighboring O ion, then we obtain $\vec{x}$ from

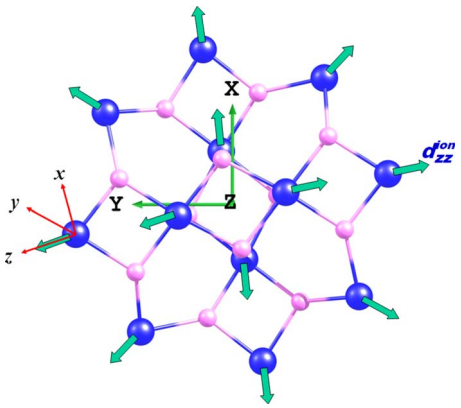

FIG. 5. (Color online) Schematic diagram showing the directions of local anisotropy in $Mn_{12}Ac$. The z component of the single-ion anisotropies of all the Mn ions are directed along the plane perpendicular to the laboratory Z axis (scheme 3).

TABLE I. D_M values of ground and excited states of $Mn_{12}Ac$ under various schemes in Kelvin. For scheme 2, we have presented the D_M values only for $\theta \sim 17°$ for which the D_M value of the ground state matches with the experimentally observed value.

State	D_M (K) Scheme 1	Scheme 2	Scheme 3
Ground state (S=10)	−0.8138	−0.7083	0.4075
First excited state (S=9) E_g=35.1 K	−0.6722	−0.6105	0.3449
Second excited state (S=8) E_g=60.4 K	−0.5009	−0.4264	0.2464

$$\vec{x} = \vec{O} - (\vec{O} \cdot \vec{z})\vec{z}. \tag{8}$$

Then, the y axis of the ion is obtained by taking the cross product of $\vec{z}$ and $\vec{x}$, $\vec{y}=\vec{z}\times\vec{x}$. These three mutually orthogonal vectors are then normalized to obtain the orthonormal set of coordinate axes x, y, and z of the ion center. The single-ion local axes are represented in the laboratory frame as

$$x = C_{i,Xx}X + C_{i,Yx}Y + C_{i,Zx}Z,$$

$$y = C_{i,Xy}X + C_{i,Yy}Y + C_{i,Zy}Z,$$

$$z = C_{i,Xz}X + C_{i,Yz}Y + C_{i,Zz}Z, \tag{9}$$

where the Cs are the direction cosines of Eq. (7) and the index i correspond to the site i. The procedure is repeated for

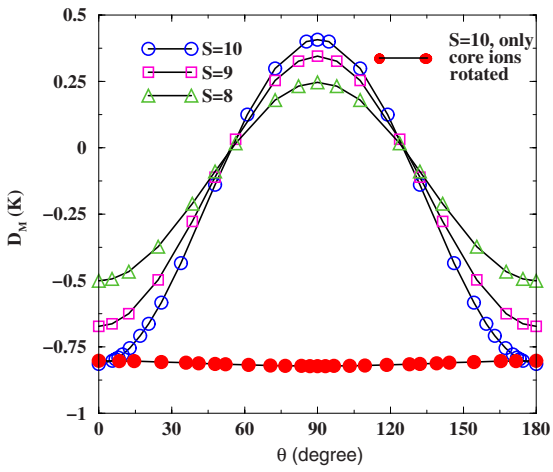

FIG. 6. (Color online) Variation of D_M as a function of θ, the angle the z component of local anisotropy of Mn(III) ions makes with the laboratory Z axis in eigenstates with total spin 10, 9, and 8. The orientation of Mn(IV) ions is kept fixed at $\sim 48°$ from the molecular Z axis. The curve with filled circles correspond to the variation of D_M when the local anisotropies of the core Mn(IV) ions only are rotated and those of Mn(III) ions are fixed along the Z axis. The variation of D_M with θ follows the equation $D_M(S) = D_M^0(S)(3\cos^2\theta - 1)$, with all $D_M^0(10) = -0.40$, $D_M^0(9) = -0.34$, and $D_M^0(8) = -0.25$. Schemes 1, 2, and 3 correspond to $\theta = 0°$, 17°, and 90°. Best fit for the experimental D_M value in the $S^{\text{total}}=10$ state corresponds to $\theta \sim 17°$.

TABLE II. Energy gaps (Δ) and D_0 values for the $S=10$ ground state corresponding to different sets of parameter values in $Mn_{12}Ac$.

S. No.	J_1 (K)	J_2 (K)	J_3 (K)	J_4 (K)	Δ (K)	D_0 (K)
1	215	85	85	−64.5	35.1	−0.40
2	215	85	85	−85	67.0	−0.43
3	215	85	64.5	−64.5	72.7	−0.46
4	215	85	45	−45	80.0	−0.49
5	215	85	−85	−45	224	−0.58

every magnetic ion to obtain coordinate axes set, x, y, and z, and the direction cosines in each case. We have obtained the magnetic anisotropy parameters D_M and E_M for $Mn_{12}Ac$ and Fe_8 clusters as a function of the angle of rotation of the local z axis with respect to the laboratory Z axis. In the following subsections, we discuss the results for the two clusters.

A. Magnetic anisotropy in $Mn_{12}Ac$ SMM

We have first obtained the ground state and few excited states of the $Mn_{12}Ac$ system by exactly solving the unperturbed Hamiltonian given in Eq. (3), using the exchange interactions shown in Fig. 1.[9] The ground state of the system corresponds to total spin 10 with a total spin 9 excited state at 35.1 K from the ground state. The second excited state occurs at 60.4 K from the ground state and corresponds to total spin 8. To obtain the molecular anisotropy values in these eigenstates, we have used different single-ion axial anisotropy values of −5.35 and 1.226 K, respectively, for Mn(III) and Mn(IV) ions. We have also introduced transverse anisotropy of 0.022 and 0.043 K for Mn(III) and Mn(IV) sites, respectively. We have studied the variation of molecular anisotropy as a function of orientation of the local anisotropies by rotating the local $\mathcal{D}$ tensor around the molecular Z axis. Scheme 1 shown in Fig. 3 corresponds to the case when all the single-ion z axes are pointed parallel to the laboratory Z direction. In scheme 2 (Fig. 5), we have fixed the orientation of the local anisotropies of the core Mn(IV) ions along the line joining the ion and the molecular center (~48° from the laboratory Z axis), while the anisotropies of the Mn(III) ions is rotated and the angle, which it makes with the molecular Z axis, is defined as θ (refer to Fig. 4). The orientation of the local anisotropy of Mn(III) ions, for which we get the best agreement with experiments, corresponds to $\theta \sim 17°$. In scheme 3 (Fig. 5), we have restricted the z component of single-ion anisotropy to the laboratory X-Y plane. We have studied the variation in the molecular anisotropies in these schemes for the ground and the excited eigenstates. We show in Table I, the D_M values for the ground and the excited spin states of the molecule for schemes 1, 2, and 3. We note that when the local anisotropies are systematically varied, there is a very large variation in the molecular anisotropy as a function of the local orientation (Fig. 6). This seems to be true for all the states of $Mn_{12}Ac$ that we have studied. We note that given the orientations of local anisotropies, the actual molecular anisotropy values are different in different spin eigenstates. This may be rationalized from the fact that the energy gaps between the ground and the excited states are large, as a consequence of which the spin correlations in these states are very different. We also note that in all cases, from the eigenvectors of the $\mathcal{D}^{(M)}$ matrix, we find that the choice of our laboratory frame is very close to the principal axis of the molecular system.

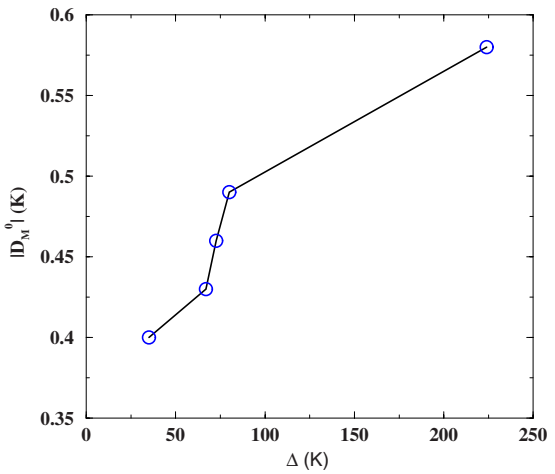

FIG. 7. (Color online) Variation of $|D_M^0|$ as a function of energy gap (Δ in Kelvin) for the $S^{total}=10$ ground state of $Mn_{12}Ac$ for parameters listed in Table II, $D_M(\theta)$ is given by $-|D_M^0|(3\cos^2\theta - 1)$.

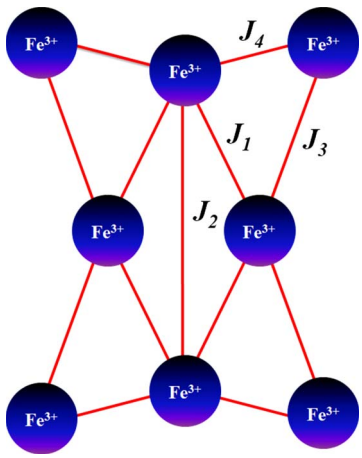

FIG. 8. (Color online) Schematic of exchange interactions in Fe_8 SMM. Js are the strength of superexchange interaction with $J_1=150$ K, $J_2=25$ K, $J_3=30$ K, and $J_4=50$ K (Ref. 9).

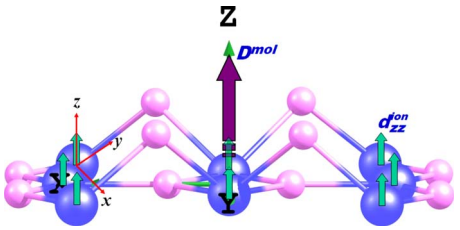

FIG. 9. (Color online) Schematic diagram showing the directions of local anisotropy in Fe_8. The single-ion anisotropies of all the Fe(III) ions are directed along the laboratory Z axis (scheme 4).

We also examined the role of magnetic orientations of the core Mn(IV) ions ($s=3/2$) and the crown Mn(III) ions ($s=2$) in determining the molecular anisotropies by fixing the single-ion orientation of the crown Mn(III) ions at 0° and rotating only the orientation of the core Mn(IV) ions systematically. The variation of D_M for the $S=10$ ground state as a function of rotation of the local anisotropies of the core Mn(IV) ions is shown in Fig. 6. We find that the molecular anisotropy is not sensitive to the local orientations of the core Mn(IV) ions, while the orientation of the crown Mn(III) ions control the variation of the molecular magnetic anisotropy in $Mn_{12}Ac$. It should be noted that, in the case of $Mn_{12}Ac$, E_M vanishes by virtue of the D_{2d} point group symmetry to which the molecule belongs. To study the variation of D_M^0 with the exchange parameters of the unperturbed Hamiltonian, we explored five different sets of exchange constants.[9] In each case, the ground state has spin $S^{\text{total}}=10$, but the gap to the lowest excited spin state varies (Table II). The lowest excited spin state has $S^{\text{total}}=9$ in all cases. We see that there is an increase in $|D_M^0|$ with increasing gap. The variation of $|D_M^0|$ with spin gap is shown in Fig. 7. We note that the magnitude of anisotropy nonuniformly increases with the gap.

B. Magnetic anisotropy in Fe_8 SMM

We have also computed the values of molecular anisotropy for the Fe_8 molecular magnet. The unperturbed Hamiltonian in Eq. (3) is exactly solved using exchange parameters, $J_1=150$ K, $J_2=25$ K, $J_3=30$ K, and $J_4=50$ K (Fig. 8).[9] The ground state of the system corresponds to total spin $S=10$ with a $S=9$ state at 13.56 K, a $S=9$ state at 27.28 K, and a $S=8$ state at 28.33 K above the ground state. To calculate the magnetic anisotropy of Fe_8, we have taken the

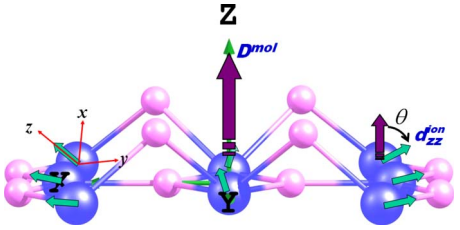

FIG. 10. (Color online) Schematic diagram showing the directions of local anisotropy in Fe_8. The z component of the single-ion anisotropies of all the Fe(III) ions are inclined at an angle θ to the laboratory Z axis (scheme 5).

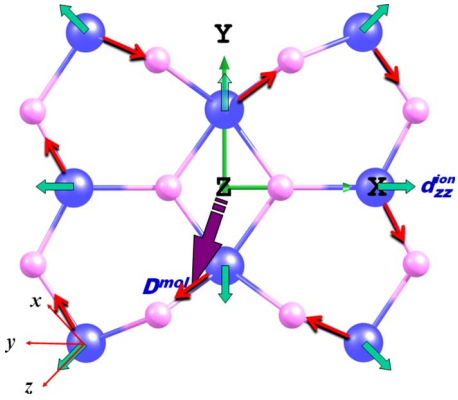

FIG. 11. (Color online) Schematic diagram showing the directions of local anisotropy in Fe_8. The z component of the single-ion anisotropies of all the Fe(III) ions are directed along the plane perpendicular to the laboratory Z axis (scheme 6). The arrows indicate the Fe-O bonds on which the chosen local x axis has maximum projection.

single-ion axial and rhombic anisotropy values for Fe(III) centers to be 1.96 and 0.008 K, respectively. Using these, we have computed the molecular anisotropy values for three schemes (schemes 4, 5, and 6) shown in Figs. 9–11. Scheme 4 corresponds to the case wherein the single-ion anisotropy of all the Fe(III) ions are pointed along the laboratory Z direction. In scheme 5, the anisotropies of the Fe(III) ions are inclined at an angle θ to the laboratory Z axis (refer to Fig. 10). In scheme 6, we have restricted the z component of single-ion anisotropy to the laboratory X-Y plane. We have studied the variation in the molecular anisotropies as a function of orientation of local anisotropy in these schemes for ground and the excited eigenstates (Fig. 12). We show in Table III the D_M values for the ground and the excited spin states of the molecule for schemes 4, 5, and 6. We note that

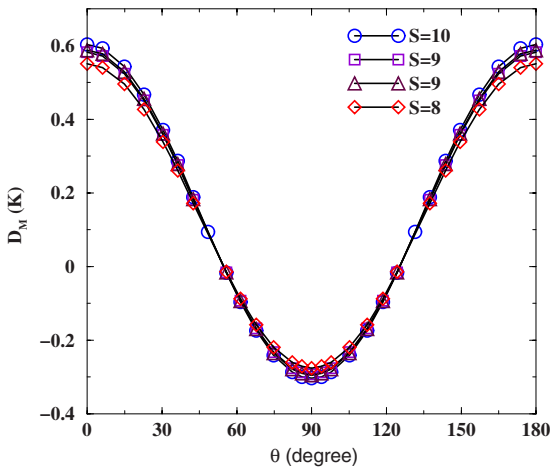

FIG. 12. (Color online) Variation of D_M in Fe_8 cluster as a function of θ, the angle the z component of local anisotropy of Fe(III) ions makes with the laboratory Z axis. All the plots can be fitted to $D_M^0(S)(3\cos^2\theta-1)$, with $D_M^0(10)=0.3$, $D_M^0(9)=0.29$, and $D_M^0(8)=0.275$. $D_M^0(S)$ is almost independent of S. Best fit for the experimental D_M value in the $S^{\text{total}}=10$ state corresponds to $\theta\sim 82°$.

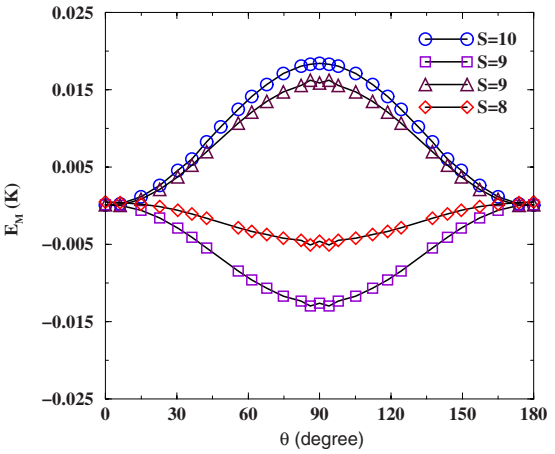

FIG. 13. (Color online) Variation of E_M in Fe_8 cluster as a function of θ, the angle the z component of local anisotropy of Fe(III) ions makes with the laboratory Z axis for scheme 5.

when the local anisotropies are systematically varied, there is a very large variation in the molecular anisotropy as a function of the local orientation (Fig. 12), similar to $Mn_{12}Ac$, in all the eigenstates that we have studied. We also note that given the orientations of local anisotropies, the actual molecular anisotropy values are not very different in different spin eigenstates since the energy gaps between the ground and the excited states are small and since the spin correlations in these states are not significantly different. The orientation of the local anisotropy centers, for which we get the best agreement with experiments (D_M=−0.28 K), corresponds to $\theta \sim 82°$.[26,27] As with $Mn_{12}Ac$, we find that the laboratory frame we have chosen is very close to molecular axis in all the cases. In case of Fe_8 cluster, the D_2 symmetry commutes with the Hamiltonian in Eq. (2) and allows for a nonzero E_M term. The variation of E_M as a function of θ is shown in Fig. 13. The value of E_M, for which D_M has the best fit, is 0.017 K compared to the experimental estimate of 0.046 K obtained from high-frequency EPR measurements.[23] In this case also, we have explored the variation of D_M^0 with the exchange constants in the unperturbed Hamiltonian [Eq. (3)].[9] Unlike with $Mn_{12}Ac$, we find that D_M^0 is almost independent of the excitation gap of the exchange Hamiltonian (Table IV).

IV. CONCLUSIONS

In this paper we presented a general method to calculate the molecular magnetic anisotropy parameters, D_M and E_M, for single molecule magnets in a chosen eigenstate of the exchange Hamiltonian. Since anisotropy is generally weak in SMMs compared to exchange interaction, we treat the anisotropy Hamiltonian as a perturbation over the exchange Hamiltonian. Calculation of D_M and E_M values, assuming only dipolar interactions between the transition metal ions, gives negligible values of molecular magnetic anisotropy compared to the experimental values. Therefore, we focus on the molecular anisotropy from the single-ion anisotropies of the individual transition metal centers in the SMM. The single-ion anisotropy has relativistic origin (spin-orbit interactions generally dominate over dipolar interactions between unpaired electrons in case of transition metal ions) and are hence short ranged with inverse cube dependence on distance. Therefore, we neglect interaction between spin moment on one ion with the orbital moment on another. This approximation simplifies the perturbation Hamiltonian. The molecular anisotropies are computed from the single-ion anisotropies using first-order perturbation theory for different spin states of the SMMs. We have computed the molecular magnetic anisotropy parameters of $Mn_{12}Ac$ and Fe_8 SMMs in various eigenstates of different total spin. We also studied the variation of molecular anisotropy by rotating the local anisotropy of the metal ions. In case of $Mn_{12}Ac$, we find that the molecular anisotropy changes drastically with the local anisotropy direction. The D_M value we have computed is different in ground and excited states, owing to a large difference in spin-spin correlation values. The molecular anisotropy of $Mn_{12}Ac$ does not change significantly with the orientation of the local anisotropy of the core Mn(IV) ions. In the case of Fe_8 cluster also, we find that the molecular an-

TABLE III. D_M values of ground and excited states of Fe_8 under schemes 4, 5, and 6 in Kelvin. For scheme 5, we have presented the D_M values only for θ=82.2° for which the D_M value of the ground state matches with the experimentally observed value.

State	D_M (K) Scheme 4	Scheme 5	Scheme 6
Ground state (S=10)	0.6030	−0.2867	−0.3033
First excited state (S=9) E_g=13.56 K	0.5821	−0.2763	−0.2923
Second excited state (S=9) E_g=27.28 K	0.5877	−0.2790	−0.2952
Third excited state (S=8) E_g=28.33 K	0.5503	−0.2607	−0.2758

TABLE IV. Energy gaps (Δ) and D_0 values for the S=10 ground state corresponding to different sets of parameter values in Fe_8.

S. No.	J_1 (K)	J_2 (K)	J_3 (K)	J_4 (K)	Δ (K)	D_0 (K)
1	180	153	22.5	52.5	5.87	0.30
2	150	25	30	50	13.56	0.30
3	195	30	52.5	22.5	41.40	0.30
4	201	36.2	58.3	26.1	42.5	0.30

isotropy parameters depend strongly on the orientation of the local anisotropy. D_M value is not very different in ground and excited states probably due to small energy gaps, which implies similar spin-spin correlations. Finally, we have computed the anisotropy constants for different choices of the exchange constants of the exchange Hamiltonian corresponding to different spin excitation gaps. We find that in $Mn_{12}Ac$, the anisotropy constants increase significantly with the gap, while in Fe_8 they are almost independent of the gap.

In case of $Mn_{12}Ac$, the first-order rhombic anisotropy term is zero due to the D_{2d} symmetry of the molecule, while it is nonzero in Fe_8. The second-order rhombic anisotropy terms commute with the molecular symmetry of the $Mn_{12}Ac$ cluster and cause tunneling between the states on either side of the double potential well. Our method can also be extended to the calculation of higher-order anisotropy constants.

ACKNOWLEDGMENTS

The authors thank Oinam Nganba Meetei for the useful discussions, Indo-French Centre for Promotion of Advanced Research (IFCPAR) under Project No. 3108-3 and Indo-Swedish Research Council under Project No. 348-2006-6666 for the financial support.

*ramasesh@sscu.iisc.ernet.in

[1] L. Thomas, F. Lionti, R. Ballou, D. Gatteschi, R. Sessoli, and B. Barbara, Nature (London) **383**, 145 (1996).
[2] W. Linert and M. Verdaguer, *Molecular Magnets: Recent Highlights* (Springer-Verlag, New York, 2003).
[3] J. S. Miller and M. Drillon, *Magnetism: Molecules to Materials IV* (Wiley, New York, 2003).
[4] M. Shoji, K. Koizumi, T. Hamamoto, Y. Kitagawa, S. Yamanaka, M. Okumura, and K. Yamaguchi, Chem. Phys. Lett. **421**, 483 (2006).
[5] K. Wieghardt, K. Pohl, I. Jibril, and G. Huttner, Angew. Chem., Int. Ed. Engl. **23**, 77 (1984).
[6] E. D. Barco, N. Vernier, J. M. Hernandez, J. Tejada, E. M. Chudnovski, E. Molins, and G. Bellessa, Europhys. Lett. **47**, 722 (1999).
[7] R. Sessoli, D. Gatteschi, A. Canneschi, and M. A. Novak, Nature (London) **365**, 141 (1993).
[8] S. Sahoo, R. Rajamani, S. Ramasesha, and D. Sen, Phys. Rev. B **78**, 054408 (2008).
[9] C. Raghu, I. Rudra, D. Sen, and S. Ramasesha, Phys. Rev. B **64**, 064419 (2001).
[10] S. Sinnecker and F. Neese, J. Phys. Chem. A **110**, 12267 (2006).
[11] J. L. Oudar and J. Zyss, Phys. Rev. A **26**, 2016 (1982).
[12] A. Bencini, C. Benelli, and D. Gatteschi, Coord. Chem. Rev. **60**, 131 (1984).
[13] A. Bencini and D. Gatteschi, *EPR of Exchange Coupled Systems* (Springer, Berlin, 1990).
[14] M. R. Pederson and S. N. Khanna, Phys. Rev. B **60**, 9566 (1999).
[15] M. R. Pederson, J. Kortus, and S. N. Khanna, J. Appl. Phys. **91**, 7149 (2002).
[16] J. Kortus, T. Baruah, N. Bernstein, and M. R. Pederson, Phys. Rev. B **66**, 092403 (2002).
[17] R. Takeda, S. Mitsuo, S. Yamanaka, and K. Yamaguchi, Polyhedron **24**, 2238 (2005).
[18] R. Takeda, K. Koizumi, M. Shoji, H. Nitta, S. Yamanaka, M. Okumura, and K. Yamaguchi, Polyhedron **26**, 2309 (2007).
[19] F. Neese and E. Solomon, Inorg. Chem. **37**, 6568 (1998).
[20] A. Carrington and A. McLachlan, *Introduction to Magnetic Ressonance: With Applications to Chemistry and Chemical Physics* (Harrer and Row, New York, 1967).
[21] S. Ramasesha and Z. G. Soos, Chem. Phys. **91**, 35 (1984).
[22] A. L. Barra, D. Gatteschi, and R. Sessoli, Chem.-Eur. J. **6**, 1608 (2000).
[23] A.-L. Barra, P. Debrunner, D. Gatteschi, C. E. Schulz, and R. Sessoli, Europhys. Lett. **35**, 133 (1996).
[24] A. Cornia, R. Sessoli, L. Sorace, D. Gatteschi, A. L. Barra, and C. Daiguebonne, Phys. Rev. Lett. **89**, 257201 (2002).
[25] A. L. Barra, D. Gatteschi, R. Sessoli, G. L. Abbati, A. Cornia, A. C. Fabretti, and M. G. Uytterhoeven, Angew. Chem., Int. Ed. Engl. **36**, 2329 (1997).
[26] S. Accorsi *et al.*, J. Am. Chem. Soc. **128**, 4742 (2006).
[27] P. ter Heerdt, M. Stefan, E. Goovaerts, A. Canneschi, and A. Cornia, J. Magn. Reson. **179**, 29 (2006).